

Growth of Ultrathin Films of Amorphous Ruthenium–Phosphorus Alloys Using a Single Source CVD Precursor

Jinhong Shin,[†] Abdul Waheed,[‡] Kyriacos Agapiou,[‡] Wyatt A. Winkenwerder,[§] Hyun-Wu Kim,[§]
Richard A. Jones,^{*,‡} Gyeong S. Hwang,^{*,§} and John G. Ekerdt^{*,§}

Texas Materials Institute, University of Texas at Austin, Austin, Texas 78750, Department of Chemistry and Biochemistry, University of Texas at Austin, Austin, Texas 78712, and Department of Chemical Engineering, University of Texas at Austin, Austin, Texas 78712

Received October 15, 2006; E-mail: rajones@mail.utexas.edu

Thin films of ruthenium metal are currently of interest for use in a number of microelectronics applications, including use as a Cu diffusion barrier and Cu seed layer due to its low resistivity ($\sim 7 \mu\Omega\cdot\text{cm}$), chemical stability, and low solubility with Cu.¹ Thin films of Ru can be grown by chemical vapor deposition (CVD) or atomic layer deposition (ALD) methods using precursors such as $(\text{Ru}_3(\text{CO})_{12})_2$,² cyclopentadienyl derivatives such as Cp_2Ru^3 or $(\text{EtCp})_2\text{Ru}$,⁴ and β -diketonates such as $\text{Ru}(\text{thd})_3^5$ ($\text{Cp} = \eta^5\text{-C}_5\text{H}_5$, $\text{EtCp} = \eta^5\text{-C}_5\text{H}_4\text{Et}$, $\text{thd} = 2,2,6,6\text{-tetramethyl-3,5-heptanedione}$). However, Ru and most metal films deposited by CVD or PVD methods follow a 3D, Vollmer–Weber growth mechanism, due to their high surface energy, and this leads to polycrystalline, columnar films. The columnar structure then permits fast Cu diffusion through grain boundaries due to the much higher diffusivity at these features than in the bulk.⁶ Controlling the microstructure of Ru films is therefore a key requirement in improving barrier performance. Changing the Ru film microstructure from polycrystalline to nanocrystalline or from polycrystalline to amorphous should eliminate or suppress the fast diffusion of Cu through grain boundaries.

We now report the CVD growth of ultrathin films of amorphous ruthenium–phosphorus alloys (RuP) using *cis*- $\text{H}_2\text{Ru}(\text{PMe}_3)_4$ ($\text{Me} = \text{CH}_3$) (**1**) as a single source precursor.⁷ It is interesting to note that all of the precursors previously employed for the CVD growth of Ru films feature ligands bound to Ru which are either hydrocarbons, carbon monoxide (CO), or oxygen donors. Thus, they all contain Ru–C or Ru–O bonds of some kind. Since ligand selection can often have a significant effect on the outcome of a CVD process, we explored the use of **1**, which contains Ru–H and Ru–P bonds. The Ru–H bond was selected to facilitate dissociative adsorption of *cis*- $\text{H}_2\text{Ru}(\text{PMe}_3)_4$, and the PMe_3 ligands were selected as potentially stable, volatile leaving groups. Surprisingly, under the growth conditions employed, highly conformal, smooth films of amorphous RuP alloys ($\text{P} = 15\text{--}20\%$) were obtained. In retrospect, growth of RuP should be anticipated since adsorbed PMe_3 has been shown to undergo complete demethylation on Ru(0001) at 500 K and the adsorbed P then reacted to form Ru_3P above 600 K.⁸ Indeed, in separate experiments, we find *cis*- $\text{H}_2\text{Ru}(\text{PMe}_3)_4$ to undergo demethylation at 560 K when adsorbed at 455 K.

The amorphous metallic alloys produced are related in some respects to bulk metallic alloys (or bulk metallic glasses, BMG).^{9–11} The amorphous nature of these materials results in the absence of crystalline defects typical of metals such as grain boundaries, dislocations, and stacking faults. They have therefore received

considerable interest for their extraordinary engineering properties such as strength, hardness, toughness, and elasticity. A variety of methods have been reported for the conversion of BMG into thin films based on physical methods. These include physical vapor deposition (PVD), magnetron sputtering, and ion beam assisted deposition (IBAD).^{10,11} Thin film growth by CVD offers several important advantages over physical growth methods, including economical scale-up, ease of operation, mild growth conditions, and the ability to achieve conformal coverage on features with high aspect ratios. While there are examples of chemical growth during electrochemical deposition,¹² there are very few examples of thin film growth of amorphous metallic alloys using CVD. This may be due to the fact that the chemical nature of the precursor is critically important to the outcome of the CVD process, and suitable precursors for these materials have simply not been developed. The few well-documented examples of amorphous metallic alloys grown by CVD include nitrides (WN ,¹³ TaN ,¹⁴ and CrMoN ¹⁵), borides (FeB ,¹⁶ NiB_x ¹⁷), carbides (TiC ¹⁸), and oxides (FeCo_xO_y ¹⁹).

Amorphous RuP films were grown in a cold-wall CVD reactor on thermally grown SiO_2 substrates at growth temperatures of 250–300 °C and 200 mTorr pressure with Ar carrier gas. The films have been characterized by X-ray photoelectron spectroscopy (XPS), tunneling electron microscopy (TEM), and X-ray diffraction (XRD) methods. XPS measurements revealed the presence of Ru and P both in the zero oxidation state (Figure 1). Thus the binding energy of the Ru $3d_{5/2}$ peak is observed at 280.0 eV for the films grown at 250 and 300 °C. The P $2p_{3/2}$ peak is at 129.8 eV, indicating P is present in elemental form and is not donating or accepting electrons with Ru.²⁰

The presence of elemental Ru and P therefore distinguishes these materials from the well-known binary phosphides of Ru such as Ru_2P , RuP_4 , and RuP_2 , which have precise stoichiometries and contain the P^{3-} phosphide anion and related species.²¹ X-ray diffraction (XRD) data show that the films have no long-range order (Figure 2), and selected area diffraction (SAD) studies confirmed the amorphous nature of the films (Figure 3).

High-resolution transmission electron microscopy (TEM) images also show that the films are generally noncrystalline, although a few small Ru crystallites ~ 5 nm in size were observed adjacent to the SiO_2 substrate. As revealed in SAD images (not shown), the XRD annealing series in Figure 2, and separately in TEM images, the films remain amorphous upon heating for 3 h at 350 °C and then begin to crystallize upon annealing at 500 °C for 30 min in vacuum. The crystallization of the metastable amorphous phase after annealing to these higher temperatures is expected.¹²

Ab initio molecular dynamics (MD) studies show Ru–P alloys with moderate P content can result in a glassy structure exhibiting topological and strong chemical short-range order. For the $\text{Ru}_{80}\text{P}_{20}$

[†] Texas Materials Institute.

[‡] Department of Chemistry and Biochemistry.

[§] Department of Chemical Engineering.

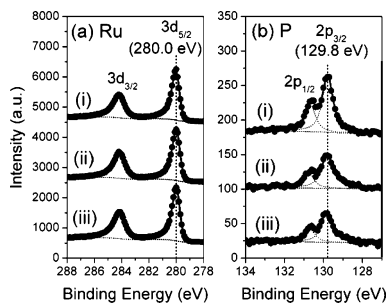


Figure 1. High-resolution XPS result of the (a) Ru 3d and (b) P 2p peaks for a film deposited at 300 °C. The spectra (i), (ii), and (iii) correspond to sputtering times of 5, 45, and 105 s, respectively. Attenuation of the P 2p peaks with depth profiling (sputtering) illustrates the concentration changing from about 28% at the surface to ~15% within the bulk.

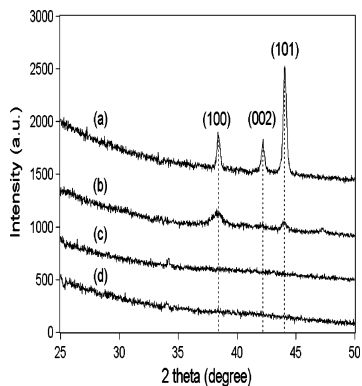


Figure 2. XRD of ~30 nm RuP deposited at 300 °C from **1**: (a) after annealing to 700 °C for 30 min, (b) after annealing to 500 °C for 30 min, (c) after annealing to 300 °C for 30 min, and (d) after growth. The (100), (002), and (101) diffraction features at 38.6, 42.4, and 44.2°, respectively, are associated with hcp Ru.

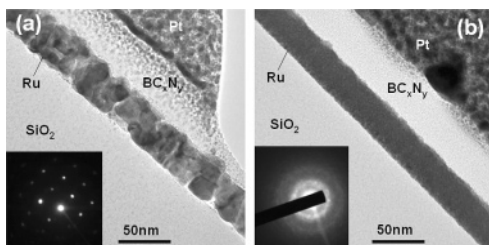


Figure 3. SAD patterns and cross section transmission electron micrographs of (a) a PVD Ru film and (b) a CVD RuP film grown at 300 °C.

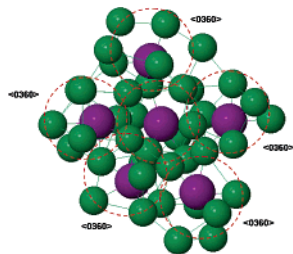


Figure 4. Modeling results for the packing of the solute-centered polyhedra for a Ru₈₀P₂₀ mixture. Large (purple) and small (green) balls represent P and Ru atoms, respectively.

structure (Figure 4), the solute coordination polyhedra preferably form the Z9 (tricapped trigonal prism) Kasper polyhedra, with a Veronoi index of $\langle 0,3,6,0 \rangle$.²² The Ru–P system also exhibits the medium-range order arising from packing the “quasi-equivalent”

P-centered Ru clusters in three-dimensional space. In fact, the short-to-medium range order is seen in other transition metal–metalloid systems where the chemical short-range order is significant.²³ Our MD simulations in the canonical ensemble were performed within the generalized gradient approximation (PW91)²⁴ to density functional theory using the Vienna ab initio simulation package.²⁵ The Ru₈₀P₂₀ alloy, with 115 Ru and 29 P atoms in a periodic supercell of volume of 2 nm³, was melted at 3500 K for 3 ps with a time step of 1 fs, and then quenched to 500 K at a rate of 1.5 K/fs, followed by static structural optimization. The structural model based on melt-quenching simulations might differ from that in experimental samples, which could also be determined by CVD kinetics. Nonetheless, our MD simulation results are sufficient to provide insight into the nature of local packing in Ru–P amorphous structures.

In summary, we describe the use of a single source precursor for the CVD growth of ultrathin films of amorphous RuP alloys. Significantly, the chemical composition of the precursor has a direct influence on both the elemental composition and morphology of the grown films. To the best of our knowledge, these films are the first CVD grown binary transition metal phosphorus amorphous alloys. Further studies are in progress.

Acknowledgment. This work was supported by the Semiconductor Research Corporation (Contract 2005-KC-1292.016), the State of Texas Advanced Materials Research Center, the National Science Foundation (Grant CTS-0553839), and the Robert A. Welch Foundation (Grant F-816).

References

- Goswami, I.; Laxman, R. *Semicond. Int.* **2004**, *27*, 49.
- Wang, Q.; Ekerdt, J. G.; Gay, D.; Sun, Y.; White, J. M. *Appl. Phys. Lett.* **2004**, *84*, 1380.
- Green, M.; Gross, M.; Papa, L.; Schnoes, K.; Brasen, D. *J. Electrochem. Soc.* **1985**, *132*, 2677.
- Matsui, Y.; Hiratani, M.; Nabatame, T.; Shimamoto, Y.; Kimura, S. *Electrochem. Solid State Lett.* **2002**, *5*, C18.
- Lashdaf, M.; Hatanpää, T.; Krause, A. O. I.; Lahtinen, J.; Lindblad, M.; Tiitta, M. *Appl. Catal. A* **2003**, *241*, 51.
- Lin, J.; Lee, C. *J. Electrochem. Soc.* **1999**, *146*, 3466.
- Jones, R. A.; Wilkinson, G.; Colquhoun, I. J.; McFarlane, W.; Galas, A. M. R.; Hursthouse, M. B. *J. Chem. Soc., Dalton Trans.* **1980**, 2480.
- Tao, H.-S.; Diebold, U.; Shinn, N. D.; Madey, T. E. *Surf. Sci.* **1997**, *375*, 257.
- Sheng, H. W.; Luo, W. K.; Alamgir, F. M.; Bai, J. M.; Ma, E. *Nature* **2006**, *439*, 419.
- Busch, R.; Hufnagel, T. C.; Eckert, J.; Inoue, A.; Johnson, W. L.; Yavari, A. R. *Mater. Res. Soc. Symp. Proc.* **2004**, 806.
- Luborsky, F. E., Ed. *Amorphous Metallic Alloys*; Butterworth-Heinemann: Woburn, MA, 1983.
- Kohn, A.; Eizenberg, M.; Shacham-Diamond, Y. *J. Appl. Phys.* **2003**, *94*, 3810.
- Kelsey, J. E.; Goldberg, C.; Nuesca, G.; Peterson, G.; Kaloyeros, A. E.; Arkles, B. *J. Vac. Sci. Technol., B* **1999**, *17*, 1101.
- Han, C.-H.; Cho, K.-N.; Oh, J.-E.; Paek, S.-H.; Park, C.-S.; Lee, S.-I.; Lee, M. Y.; Lee, J. G. *Jpn. J. Appl. Phys. Part 1* **1998**, *37*, 2646.
- Tenhover, M. *Mater. Res. Soc. Symp. Proc.* **1995**, *363*, 257.
- Jun, C.-S.; Fehlner, T. P.; Long, G. L. *Chem. Mater.* **1992**, *4*, 440.
- Mullendore, A. W. U.S. Patent Appl. 170228, 1989.
- Alloca, C. M.; Williams, W. S.; Kaloyeros, A. E. *J. Electrochem. Soc.* **1987**, *134*, 3170.
- Czekaj, C. L.; Geoffroy, G. L. *Inorg. Chem.* **1988**, *27*, 8.
- Li, H.; Dai, W.; Wang, W.; Fang, Z.; Deng, J. *Appl. Surf. Sci.* **1999**, *152*, 25.
- Wells, A. F. *Structural Inorganic Chemistry*, 5th ed.; Oxford University Press: Oxford, 1986; pp 840–841.
- Finney, J. L. *Nature* **1977**, *266*, 309.
- Sheng, H. W.; Luo, W. K.; Alamgir, F. M.; Bai, J. M.; Ma, E. *Nature* **2006**, *439*, 419.
- Perdew, J. P.; Chevary, J. A.; Vosko, S. H.; Jackson, K. A.; Pederson, M. R.; Singh, D. J.; Fiolhais, C. *Phys. Rev. B* **1992**, *46*, 6671.
- Kresse, G.; Furthmüller, J. *Phys. Rev. B* **1996**, *54*, 11169.

JA0673938